Langmuir

Article

pubs.acs.org/Langmuir

Surface Modification of a Biodegradable Magnesium Alloy with Phosphorylcholine (PC) and Sulfobetaine (SB) Functional Macromolecules for Reduced Thrombogenicity and Acute Corrosion Resistance

Sang-Ho Ye,[†,‡] Yong-Seok Jang,[⊥] Yeo-Heung Yun,[⊥] Venkat Shankarraman,[†,‡] Joshua R. Woolley,[†,§] Yi Hong,[†,‡,○] Lara J. Gamble,[#] Kazuhiko Ishihara,[¶] and William R. Wagner*[,†,‡,§,∥]

[†]McGowan Institute for Regenerative Medicine, [‡]Department of Surgery, [§]Department of Bioengineering, and [∥]Department of Chemical Engineering, University of Pittsburgh, Pittsburgh, Pennsylvania 15219, United States

[⊥]Department of Bioengineering, North Carolina Agricultural & Technical State University, Greensboro, North Carolina 27411, United States

[#]Department of Bioengineering and NESAC/BIO, University of Washington, Seattle, Washington 98195, United States

[¶]Department of Materials Engineering, School of Engineering, The University of Tokyo, 7-3-1, Hongo, Bunkyo-ku, Tokyo 113-8656, Japan

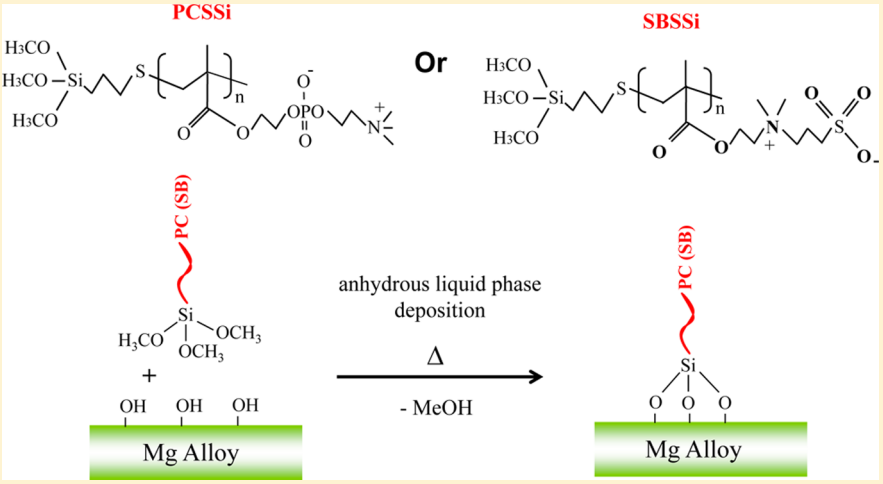

ABSTRACT: Siloxane functionalized phosphorylcholine (PC) or sulfobetaine (SB) macromolecules (PCSSi or SBSSi) were synthesized to act as surface modifying agents for degradable metallic surfaces to improve acute blood compatibility and slow initial corrosion rates. The macromolecules were synthesized using a thiol-ene radical photopolymerization technique and then utilized to modify magnesium (Mg) alloy (AZ31) surfaces via an anhydrous phase deposition of the silane functional groups. X-ray photoelectron spectroscopy surface analysis results indicated successful surface modification based on increased nitrogen and phosphorus or sulfur composition on the modified surfaces relative to unmodified AZ31. In vitro acute thrombogenicity assessment after ovine blood contact with the PCSSi and SBSSi modified surfaces showed a significant decrease in platelet deposition and bulk phase platelet activation compared with the control alloy surfaces. Potentiodynamic polarization and electrochemical impedance spectroscopy data obtained from electrochemical corrosion testing demonstrated increased corrosion resistance for PCSSi- and SBSSi-modified AZ31 versus unmodified surfaces. The developed coating technique using PCSSi or SBSSi showed promise in acutely reducing both the corrosion and thrombotic processes, which would be attractive for application to blood contacting devices, such as vascular stents, made from degradable Mg alloys.

1. INTRODUCTION

While biodegradable polymers are broadly employed for a variety of medical devices, the use of similarly labile metallic materials has not found widespread use clinically. Only in recent years has the interest in bioabsorbable metallic alloys been reinvigorated after early pioneering experiments with these materials over 125 years ago.[1] Dominated so far by magnesium-based alloys, research into degradable metal devices

Received: April 9, 2013
Revised: May 17, 2013
Published: May 24, 2013

   dx.doi.org/10.1021/la401341y | *Langmuir* 2013, 29, 8320−8327

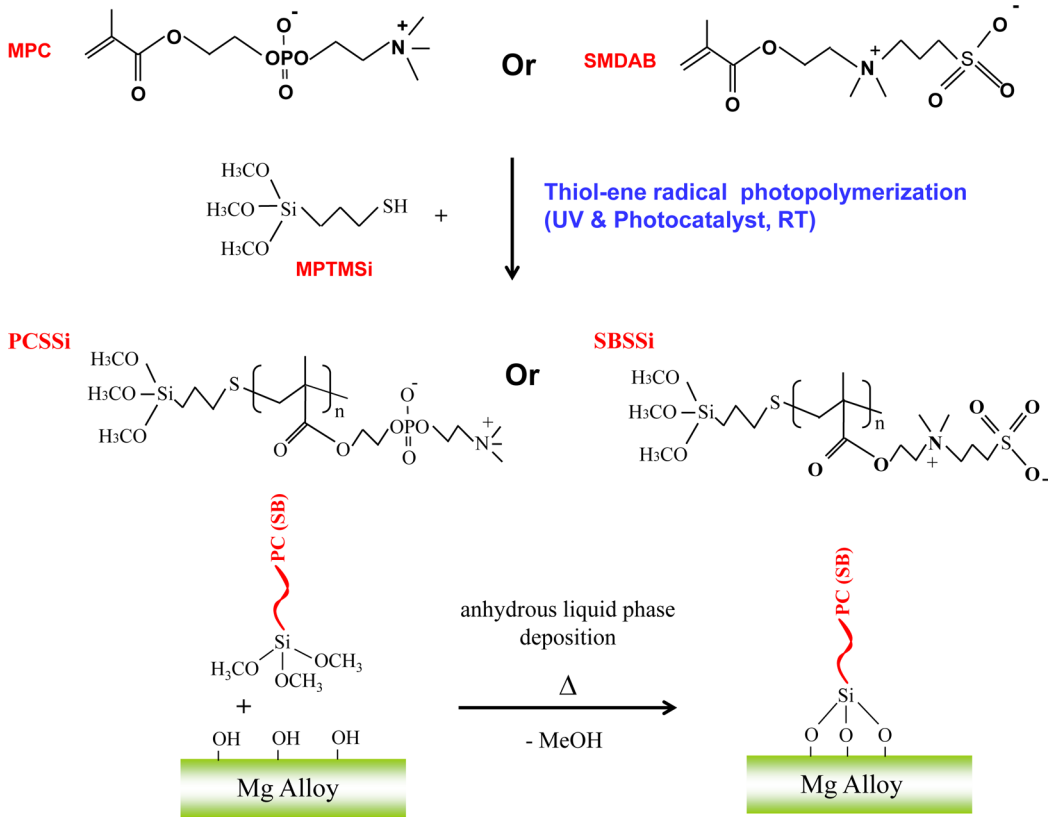

Figure 1. PCSSi and SBSSi structure and schematic for surface modification.

has recently reached the level of clinical investigation, and interest in applying these materials in a number of different settings from orthopedic to cardiovascular systems is growing.[2] For blood contacting applications, such as with an arterial stent, the hemocompatibility of the metallic alloy is a primary concern, particularly in terms of avoiding thrombotic deposition in the early period after the stent is placed. Yet the underlying mechanical properties, processability and degradation rate of an otherwise attractive alloy, may not possess ideal levels of thromboresistance. As a result, the potential to surface modify magnesium-based alloys to improve hemocompatibility in the early period when the thrombotic risk is highest and prior to the onset of substantial degradation is of particular interest.[3,4]

A number of different coating approaches might be taken to improve the surface biocompatibility of Mg-based alloys. Treatment of the metal through oxidation or ion implantation, polymeric film coatings, and direct molecular attachment have all been explored.[5,6] To achieve reduced thrombogenicity on nondegradable metallic surfaces, as well as in polymeric systems, phosphorylcholine (PC)-based or sulfobetaine (SB)-based modifications have been shown to be effective.[7−16] The zwitterionic PC or SB groups putatively act to reduce the driving force for protein adsorption, thus reducing the capacity for cell adhesion and improving thromboresistance.[17−19]

Our objective in this study was to design and synthesize siloxane functional PC or SB macromolecules using a thiol-ene radical photopolymerization technique[20−23] that would then be applied to achieve surface modification of a Mg alloy with PC or SB macromolecules in a simple, one-step method that could be translated to complex geometries. The macro-PC or SB modifiers with a siloxane group were attached directly on a commonly studied biodegradable Mg alloy (AZ31) using an anhydrous surface deposition method.[24] The effectiveness of the modified macro PC or SB modifiers on Mg alloy surfaces was evaluated in terms of the ovine platelet activation and adhesion from whole blood and in vitro corrosion resistance.

2. MATERIALS AND METHODS

2.1. Materials. Mg−Al−Zn alloy (AZ31; 3% Al, 1% Zn) was purchased from Goodfellow Corp. (Oakdale PA). 2-Methacryloyloxyethyl-phosphorylcholine (MPC) was obtained from NOF Corporation (Tokyo, Japan). *N*-(3-Sulfopropyl)-*N*-(methacryloxyethyl)-*N*,*N*-dimethylammonium betaine (SMDAB), 3-mercaptopropyl trimethoxysilane (MPTMSi), and benzophenone were purchased from Sigma-Aldrich (St. Louis, MO) and used as received.

2.2. Synthesis of Silanated Macro Modifier. To synthesize a macro PC surface modifier with siloxane functional groups (PCSSi, Figure 1), MPTMSi and MPC at a defined molar ratio (MPC/MPTMSi = 5:1) were dissolved with anhydrous methanol (10 mL) in a round-bottom flask equipped with a magnetic stirrer after adding a photoinitiator (benzophenone). After argon injection for 5 min to remove the air, the flask containing the reaction mixture was sealed and placed under a high intensity UV lamp (1150 V, 60 Hz, 2.5 A, wavelength: 365 nm, UVP Model B 100AP, Upland, CA) at 15 cm gap and remained at room temperature for 15 h. After the reaction, anhydrous diethyl ether and chloroform mixed solution (1:1) was used for precipitation of the synthesized product. The obtained white gel-like product (PCSSi) was further washed with anhydrous chloroform by stirring for 24 h to remove unreacted MPTMSi or MPC and dried under vacuum. A macro SB surface modifier with siloxane functional groups (SBSSi) was also synthesized with the same process as described for PCSSi synthesis. For SBSSi synthesis, trifluoroethanol (TFE) was used as the solvent for the reaction, and the product was precipitated in anhydrous MeOH and chloroform mixed solution (1:1). The synthesized SBSSi was further washed with anhydrous MeOH to remove any unreacted MPTMSi and SMDAB.

dx.doi.org/10.1021/la401341y | *Langmuir* 2013, 29, 8320−8327

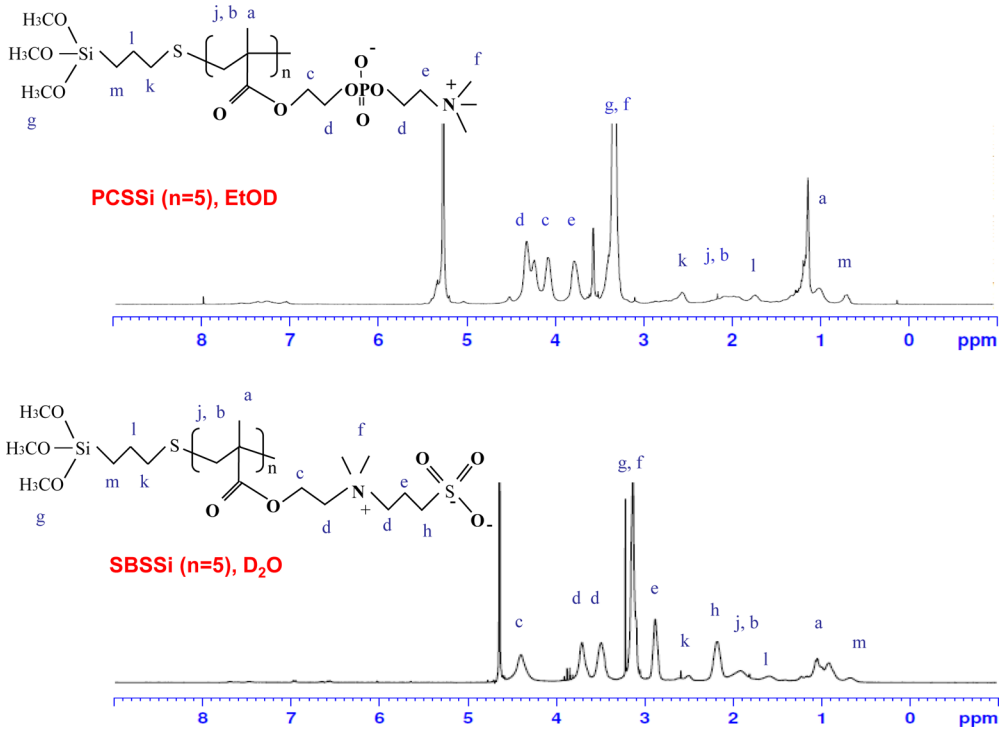

Figure 2. ^{1}H NMR spectra of the synthesized PCSSi and SBSSi.

2.3. Preparation of Surface Modified Mg Samples. AZ31 plates (1 × 1 cm or 6.35 mm diameter discs) were polished with up to 1200 grit of silicone carbide sand paper and then cleaned with acetone and trichloroethylene. The cleaned and dried samples were passivated by immersing in distilled water for 10 min and dried under vacuum. A UV/ozone treatment was applied for 30 min on the alloy surface using a UV-ozone cleaner (Novascan Tech. Inc. PSD Pro-UV, Ames, IA) to increase the surface reactivity. Then, the alloys were modified by immersing in solutions of PCSSi or SBSSi in toluene/TFE mixed solution (1:1), with triethylamine as a catalyst for 4 h at 40 °C (Figure 1).

2.4. Surface Analysis and in Vitro Blood Contacting Test. The surface composition of the modified and unmodified Mg alloy samples was analyzed by X-ray photoelectron spectroscopy (XPS) using a Surface Science Instruments S-probe spectrometer with a takeoff angle of 55° (~50 Å sampling depth) at the University of Washington (Seattle, WA).[14] The static water contact angle on the Mg alloy surfaces was measured at multiple steps through the processing: freshly polished, water contacted for 10 min, UV/ozone treated, and PCSSi or SBSSi modified, each at room temperature using a contact angle goniometer (VCA optima, AST Product Inc., Billerica, MA) and placing 1 μL of distilled water on the surfaces.

Whole blood was collected from healthy ovines by jugular venipuncture after discarding the first 3 mL. Institutional animal care and use committee (IACUC) guidelines for the care and use of laboratory animals were observed. The acute in vitro blood biocompatibility of the modified surfaces was evaluated under continuous rocking at 37 °C in freshly drawn, anticoagulated (3.0 U/mL of heparin) ovine blood for 2 h. After blood contact, the test surfaces were rinsed with PBS and immersed in a 2.5 wt % glutaraldehyde in distilled water for 15 min. Then, the surfaces were rinsed with distilled water and freeze-dried to observe the thrombotic deposition by scanning electron microscopy (SEM). The thrombotic coverage on the surfaces was evaluated using Image-J software (NIH) with selected representative electron micrographs. The percent area covered by thrombotic adhesion was calculated by image processing after image optimization by background subtraction and threshold adjustment. In addition, activated platelets in the bulk phase of the contacting blood for each sample were quantified by a flow cytometric assay after continuous rocking for 1 h at 37 °C. This assay utilized fluorescein-conjugated Annexin V binding[25] to detect and count the fraction of platelets activated to a state where the membrane was capable of binding this protein. Relative activation levels were calculated by subtracting the % activated platelets in blood from a rocked tube into which no test surface was placed.

2.5. Electrochemical Corrosion Analysis. Potentiodynamic polarization and electrochemical impedance spectroscopy (EIS) were utilized to evaluate the corrosion behavior of PCSSi or SBSSi macromolecule modified Mg alloy samples (AZ31-PCSSi or AZ31-SBSSi). The test samples were mounted in an epoxy resin with an exposed metallic area of 0.316 cm^2 and electrical connectivity accomplished by a copper wire attached to the opposite side from the exposed surface. A platinum wire was used as the counter electrode, and an Ag/AgCl electrode served as the reference electrode using a potentiostat (Gamry Instruments, USA). Electrochemical measurements were carried out in a simulated body fluid (SBF) solution with modified (AZ31-PCSSi or AZ31-SBSSi) and the AZ3l control samples as the working electrodes. The SBF solution was composed of 8 g/L NaCl, 0.4 g/L KCl, 0.14 g/L $CaCl_2$, 0.35 g/L $NaHCO_3$, 1g/L $C_6H_{12}O_6$, 0.2 g/L $MgSO_4{\cdot}7H_2O$, 0.09 g/L KH_2PO_4, and 0.06 g/L $Na_2HPO_4{\cdot}7H_2O$, following a previously described procedure.[26] Each sample was immersed in the SBF solution for 5 min to keep a stable open circuit potential. After that, the EIS measurement was performed at the open circuit potential. The amplitude of the applied AC signal was 10 mV rms, and the measured frequencies ranged from 100 kHz to 1 Hz. Potentiodynamic polarization tests were carried out at the open circuit potential as well and scanned from −0.1 V/E_{ocp} to +0.5 V/E_{ocp} at a scan rate of 5 mV/s.

2.6. Statistical Analyses. Data are presented as means with standard deviations or as medians if the data were not normally distributed. Statistical significance between sample groups was determined using ANOVA with posthoc Neuman−Keuls testing for normally distributed data, or for non-normally distributed data, nonparametric testing (independent-samples Kruskal−Wallis test) with SPSS software (IBM SPSS Statistics 20). Statistical significance was considered to exist at $p < 0.05$.

dx.doi.org/10.1021/la401341y | Langmuir 2013, 29, 8320−8327

Table 1. Atomic Percentages for Mg Alloy Surfaces at Listed Binding Energies (eV) As Determined by X-ray Photoelectron Spectroscopy

	C 1s at 285 eV	O 1s at 532 eV	Mg 2p at 50 eV	Al 2p at 74 eV	Si 2p at 106 eV	N 1s at 403 eV	P 2p at 133 eV	S 2p at 168 eV
AZ31-control	31.9 (±4.7)	44.6 (±3.0)	20.5 (±4.4)	1.3 (±0.8)	0.9 (±0.8)	0.1 (±0.2)	0.0 (±0.0)	0.2 (±0.2)
AZ31-PCSSi	38.5 (±5.4)	39.5 (±2.1)	14.4 (±2.0)	1.2 (±1.5)	2.7 (±1.6)	1.5 (±0.4)[a]	1.6 (±0.9)[a]	0.7 (±0.4)
AZ31-SBSSi	41.1 (±3.9)	33.7 (±3.4)	11.7 (±4.2)	0.3 (±0.2)	2.2 (±1.3)	1.2 (±0.3)[a]	0.2 (±0.2)	2.6 (±0.6)[a]

[a] $p < 0.05$ vs AZ31 control ($n = 4$, mean ± standard deviation).

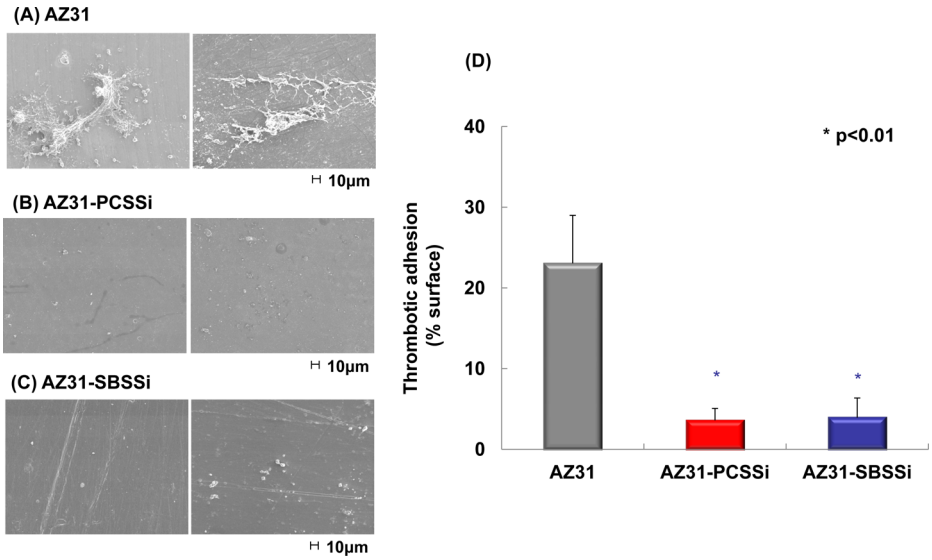

Figure 3. Electron micrographs of Mg alloy samples (A) AZ31, (B) AZ31-PCSSi, and (C) AZ31-SBSSi after contact with ovine blood for 2 h, and (D) summary of thrombotic deposition coverage of the five surfaces.

3. RESULTS

3.1. Synthesis of PCSSi and SBSSi and Surface Modification of Mg Alloy. The chemical structure of the synthesized siloxane functional PC and SB macromolecules (PCSSi and SBSSi) was confirmed by ^{1}H NMR spectroscopy (Figure 2). For PCSSi in deuterated ethanol (EtOD), the peaks were δ (ppm) = 0.60−0.82 ($SiC\underline{H}_2CH_2$), 0.90−1.35 (α-CH_3), 1.61−1.81 ($SiCH_2C\underline{H}_2$), 1.85−2.31 ($SC\underline{H}_2C$ and $C\underline{H}_2C$), 2.44−2.66 ($CH_2C\underline{H}_2S$), 3.20−3.50 ($CH_2N(C\underline{H}_3)_3$ and $Si(OC\underline{H}_3)_3$,) 3.68−3.90 ($C\underline{H}_2N(CH_3)_3$), 4.00−4.18 ($OC\underline{H}_2$), and 4.18−4.48 ($C\underline{H}_2PO_4C\underline{H}_2$), and for SBSSi in deuterium oxide (D_2O) the peaks were δ (ppm) = 0.55−0.80 ($SiC\underline{H}_2CH_2$), 0.80−1.30(α-CH_3), 1.45−1.71 ($SiCH_2C\underline{H}_2$), 1.75−2.11 ($SC\underline{H}_2C$ and $C\underline{H}_2C$), 2.08−2.28 ($CH_2C\underline{H}_2SO_3$), 2.41−2.68 ($CH_2C\underline{H}_2S$), 2.82−2.86 ($C\underline{H}_2CH_2SO_3$), 3.02−3.28 ($N(C\underline{H}_3)_2$ and $Si(OC\underline{H}_3)_3$), 3.40−3.83 ($C\underline{H}_2N(CH_3)_2C\underline{H}_2$), and 4.21−4.55 ($OC\underline{H}_2$). The degree of polymerization for the PCSSi and SBSSi molecules was 5.6 (M_w = 1840) and 5.1 (M_w = 1610), respectively, which was estimated by the peak integration ratio of $OC\underline{H}_2N$ (PC or SB groups) and $SiC\underline{H}_2$ (siloxane group) originating from each of the components on the NMR charts (Figure 2). The degree of polymerization could be controlled by the initial monomer feed ratio. For instance, using an MPC/MPTMSi molar ratio of 1:1 yielded a PCSSi with a degree of polymerization of 1.8, and using an MPC/MPTMSi molar ratio of 3:1 yielded a PCSSi with a degree of polymerization of 3.4.

The surface contact angles on Mg alloy surfaces varied significantly depending on surface treatment and modification with PCSSi or SBSSi. The water contact angle on polished and cleaned AZ31 (40.4 ± 5.7°) was significantly reduced after surface passivation with water to 18.5 ± 3.4° and UV/ozone treatment to 10.1 ± 5.5°. The contact angles on PCSSi or SBSSi modified AZ31 surfaces were also significantly reduced versus AZ31 to 12.2 ± 2.9° and 26.3 ± 2.2°, respectively ($p < 0.05$, $n = 5$). Furthermore, XPS analysis data (Table 1) were consistent with the modification of Mg alloy surfaces with the PCSSi or SBSSi based on the increased phosphorus composition on the PCSSi modified surfaces (P = 1.6 ± 0.9% on AZ31-PCSSi) and increased sulfur on the surfaces of AZ31-SBSSi (S = 2.6 ± 0.6%) in comparison to unmodified AZ31 ($p < 0.05$, $n = 4$). An elevation in Si was also observed for the modified surfaces, although this was not found to be statistically significant, and substantial variance was associated with Si amounts on the unmodified surfaces consistent with previous reports.[14]

3.2. Ovine Blood Contact. Figure 3 shows the surface morphology observed after the contacting of test surfaces with fresh ovine blood. Electron microscopy shows consistent deposition of platelets on unmodified AZ31 after blood contact with the deposited platelets in large aggregates and spread morphology (Figure 3A). In contrast, platelet deposition was sparse on the AZ31-PCSSi and AZ31-SBSSi surfaces, and it was difficult to detect large platelet aggregates on the surfaces (Figures 3B,C). Overall, surface deposition was significantly decreased on the modified surfaces versus the unmodified AZ31 control ($p < 0.01$, $n = 5$) as evaluated by Image-J software (Figure 3D). Platelet activation in the bulk phase was decreased in the blood contacted with AZ31-PCSSi (3.7 ± 1.7%) and AZ31-SBSSi (2.7 ± 1.9%), compared to the AZ31 control (7.7 ± 1.5%) ($p < 0.05$, $n = 5$).

dx.doi.org/10.1021/la401341y | Langmuir 2013, 29, 8320−8327

3.3. In Vitro Corrosion Properties of Modified Surfaces. In Figure 4 a Nyquist plot for AZ31 control and

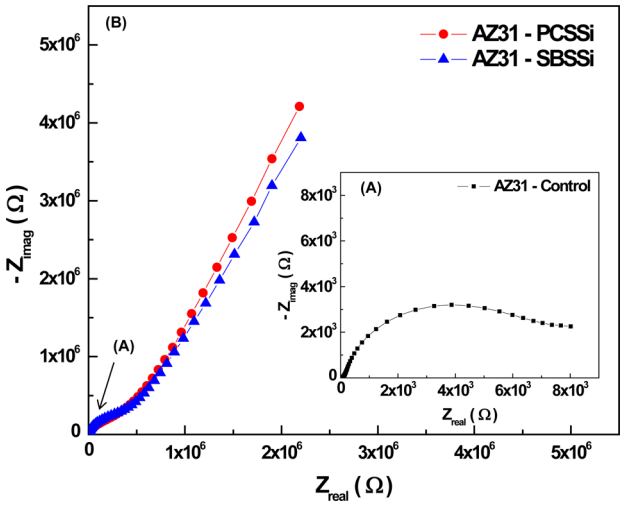

Figure 4. Nyquist plot of electrochemical impedance spectroscopy (EIS) for (A) AZ31 control and (B) the modified samples AZ31-PCSSi and AZ31-SBSSi in a simulated body fluid.

PCSSi and SBSSi modified samples in SBF solution is presented. An equivalent circuit model (ECM) shown in Figure 5 was used to fit the EIS results. This model comprised

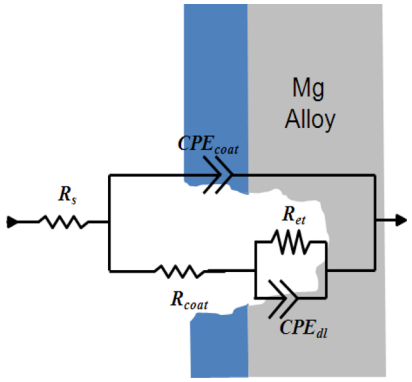

Figure 5. Equivalent circuit model used for fitting experimental EIS spectra; R_s = solution resistance, R_{coat} = coating resistance, CPE_{coat} = constant phase element of coated structure, R_{et} = electron transfer resistance, and CPE_{dl} = constant phase element of double layer.

solution resistance (R_s), coating resistance (R_{coat}), constant phase element of the coated structure (CPE_{coat}), electron transfer resistance (R_{et}), and constant phase element of double layer capacitance (CPE_{dl}). For AZ31 samples, a magnesium hydroxide layer is naturally formed and was modeled as a new time constant (CPE_{coat}, corresponding capacitance) and magnesium hydroxide resistance (R_{coat}). In the case of the PCSSi or SBSSi modified AZ31 samples, R_{coat} and CPE_{coat} were utilized as corrosion-resistance coating layers. Figure 4 shows a typical example of Nyquist plots for control and coated AZ31 samples. Nyquist results from both the control and coated samples show two time constants; one resulted from pretreatment and the other resulted from electron transfer resistance.[27] However, the diameter of the semicircles for coated samples (Figure 4B) was much larger than the diameter of the semicircle for control sample (Figure 4A), implying formation of a high corrosion resistance coating on the surface. The initial coating resistances (R_{coat}, n = 3 median) and the electron transfer resistance (R_{et}, n = 3 median) obtained from Figure 4 are summarized in Table 2. Both the initial R_{coat} and R_{et} on AZ31-PCSSi and AZ31-SBSSi surfaces was markedly higher than for AZ31 control surfaces ($p < 0.01$).

Figure 6 shows the potentiodynamic polarization curves for the AZ31 and modified surfaces in SBF solution. For AZ31, a

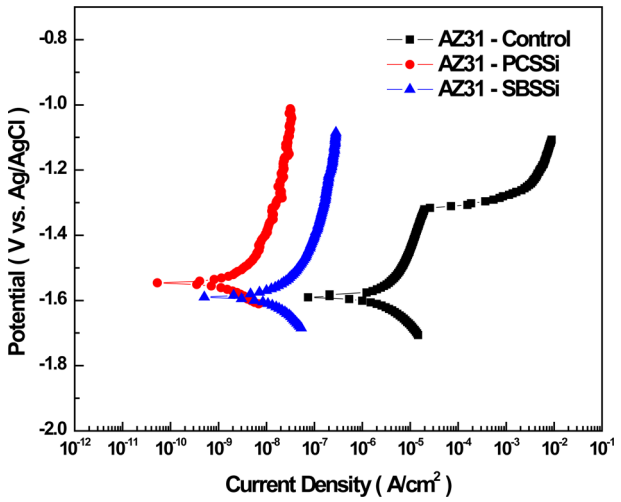

Figure 6. Potentiodynamic polarization curves of AZ31 control and the modified samples AZ31-PCSSi and AZ31-SBSSi in a simulated body fluid.

pitting corrosion point was observed in the polarization curve (E_{pit}: −1.32 V in Figure 6); however, the modified samples (AZ31-PCSSi and AZ31-SBSSi) did not appear to experience pitting corrosion, and the curves for the modified samples were shifted to a lower corrosion current density. The corrosion potential (E_{corr}) and corrosion current density (I_{corr}) of the samples acquired from the potentiodynamic polarization curves

Table 2. Coating Resistance (R_{coat}) and Electron Transfer Resistance (R_{et}) of AZ31, AZ31-PCSSi, and AZ31-SBSSi with Immersion Time in a SBF Solution[a]

samples	resistance (ohms)	initial	1 days	2 days	3 days	4 days	8 days
AZ31-control	R_{coat}	2.02×10^2	1.96×10^3	1.39×10^3	9.55×10^2	1.99×10^3	1.63×10^3
	R_{et}	1.88×10^4	1.05×10^5	1.04×10^5	8.90×10^4	1.08×10^5	1.13×10^5
AZ31-PCSSi	R_{coat}	4.74×10^5	2.90×10^5	2.87×10^5	2.86×10^5	2.64×10^5	4.77×10^3
	R_{et}	9.83×10^8	8.40×10^7	1.28×10^8	3.92×10^6	4.30×10^6	7.98×10^4
AZ31-SBSSi	R_{coat}	1.21×10^6	2.63×10^4	5.16×10^3	1.00×10^4	1.01×10^4	1.44×10^4
	R_{et}	5.63×10^{11}	6.59×10^{11}	3.25×10^{11}	9.11×10^6	6.90×10^7	3.20×10^6

[a] n = 3, median.

dx.doi.org/10.1021/la401341y | Langmuir 2013, 29, 8320−8327

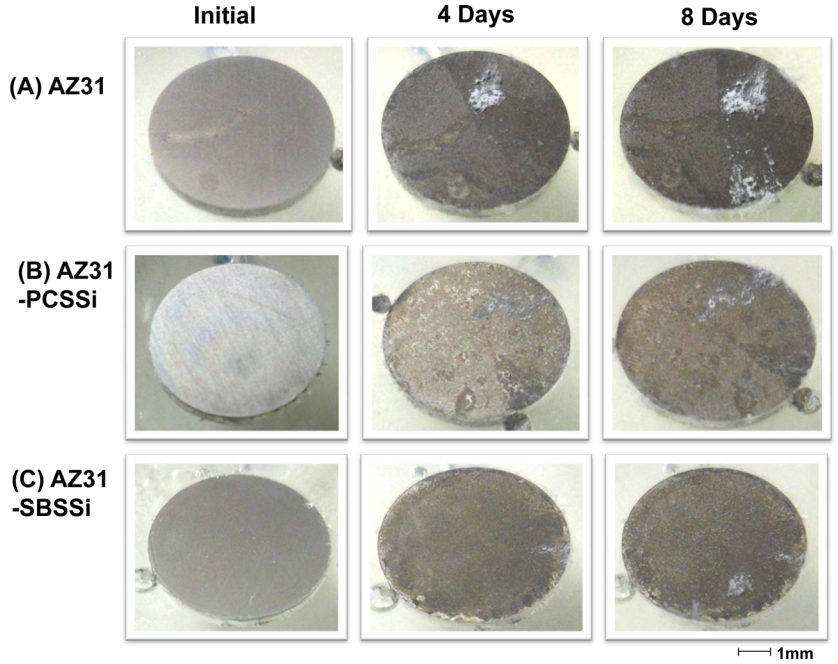

Figure 7. Macroscopic surface observation of AZ31-control, AZ31-PCSSi, and AZ31-SBSSi surfaces with immersion time in a simulated body fluid.

of Figure 6 show that the average corrosion potential (E_{corr}, n = 6, median) for the modified samples (AZ31-PCSSi (1.52 ± 0.08 V) and AZ31-SBSSi (1.63 ± 0.02 V)) did not significantly vary with respect to the control samples (1.58 ± 0.03 V). However, both modified samples had significantly lower I_{corr} values (AZ31-PCSSi (4.82×10^{-9} A/cm^2) and AZ31-SBSSi (6.78×10^{-8} A/cm^2)) than the AZ31 control (1.93×10^{-5} A/cm^2) ($p < 0.01$, n = 6, median).

The surface corrosion performance and coating resistance were also investigated with immersion time in SBF solution at 37 °C for 8 days (Figure 7 and Table 2). For the control AZ31 surface (Figure 7A), white areas of adherent corrosion byproducts were apparent by day 4, and these further spread at day 8 of Figure 7A. For the PCSSi- or SBSSi-modified samples for at least the first 4 days, limited or no white regions were seen although by day 8 some areas became apparent (Figure 7B,C). The changes in coating resistances (R_{coat}) and electron transfer resistance (R_{et}) with immersion time are summarized in Table 2. For PCSSi- or SBSSi-modified surfaces both of the R_{coat} and R_{et} was elevated with respect to AZ31 control surfaces for at least 4 days of immersion time, although the R_{coat} and R_{et} values became similar at the 8 day time point (Table 2).

4. DISCUSSION

In this study, we utilized a thiol-ene radical photopolymerization technique to prepare siloxane functionalized PC or SB macromolecules. Both radical-mediated and base/nucleophile-initiated thiol-ene reactions have been widely employed in polymer and materials synthesis to design complex or versatile functional macromolecules.[28] In the most similar approaches to the current study, Matsuno et al.[29] prepared a series of alkanethiol-S-PC surfactants via Michael-type addition of the methacrylate and alkane thiol compounds using a base catalyst, diisopropylamine. Also, Zhou et al.[30] synthesized silane-terminated functionalized polystyrene and polymethylmethacrylate polymers through radical chain-transfer polymerization with a thermal initiator, 2,2′-azobisisobutyronitrile, and prepared the self-assembled films on a silicon wafer. This thermal polymerization technique is not well-suited to control homopolymerization via radical chain growth.[31] Tucker-Schwartz et al.[32] used a photoinitiated thiol-ene click reaction to prepare functional trialkoxysilane for surface coating applications on iron oxide superparamagnetic nanoparticles, although not to form functional macromolecules or polymers.

An alternative thiol-ene radical photopolymerization technique has been investigated by a number of researchers[20−23] where a high conversion rate could be obtained by controlling the initial feed ratio of thiol, methacrylate monomer, and photoinitiator.[20] To control the initiation and the polymerization steps in the current study, we used a benzophenone, a hydrogen abstraction type of photoinitiator (a Type II photoinitiator),[33] and recognized that it might also be necessary to control the process by controlling the feed of the initiator, thiol (MPTMSi), and methacrylate (MPC or SMDAB) to minimize byproducts from the termination reaction. Further detailed studies would be needed to verify the degree to which the method utilized provided control over the various undesirable reactions.

The metal oxide surface modification using functionalized PC or SB macromolecules (PCSSi or SBSSi macromodifiers) was attractive due to the simplicity of both surface modifier synthesis and surface modification compared with previous approaches.[14−16] Thus, this described approach offers relative ease of development and application for complex surface shapes associated with some metallic devices as well as biodegradable metallic surfaces. Further, the surface modification is amenable to application under both aqueous and anhydrous conditions, the latter of which may be desirable in the processing of degradable metal systems. In this study, we have used a relatively short chain length (n = 5) of PCSSi and SBSSi macromolecules and attempted to optimize the grafting condition by adding UV/ozone treatments, which could create further hydroxyl groups on the surfaces after cleaning the Mg surfaces and oxidation with water. The effect of UV/ozone treatment was verified by contact angle measurement (data not

dx.doi.org/10.1021/la401341y | Langmuir 2013, 29, 8320−8327

shown) where it was found that 30 to 60 min of treatment was most effective to increase hydrophilicity. However, the ultimate stability of the attached macromolecules might depend on the stability of Mg oxide layer of the substrate. Therefore, the stability of the modification might be controlled by using a further surface pretreatment method to specifically generate a more stable oxide layer such as anodization,[34] alkaline heat treatments,[35] or microarc oxidation.[36] While surface composition analysis (Table 1) clearly showed the presence of PCSSi and SBSSi on the modified alloys, comparisons between the coating types were not statistically conclusive in terms of which material may have relatively better masking of the underlying material. Further studies into methods to increase surface coverage may be warranted.

There are several approaches found in the literature related to the surface modification or coating of Mg-based materials to increase corrosion resistance for potential biomedical applications.[5,6] However, only a few of these approaches were reported to improve the blood compatibility. Gu et al.[37] investigated the effect of alloying elements used with Mg on in vitro cytotoxicity and hemocompatibility, showing that hemolysis and platelet adhesion decreased significantly on Mg alloys with 1 wt % of elements such as In, Mn, Si, and Y relative to pure Mg. Unmodified Mg alloy (WE42) was found to have longer clotting times (and thus potentially improved blood biocompatibility) than the same alloy modifed with microarc oxidation or polylactide coating. The modified surface clotting time did not vary markedly from that of stainless steel (316L).[38] Hansi et al.[39] also showed that platelet adhesion on a 316L stainless steel stent was higher than for Mg alloy stents. Li et al.[40] showed that hemolysis on WE43 magnesium alloy was significantly decreased after depositing a SiC film by a plasma enhanced chemical deposition technique.

The data reported in the current study show that surface modification with the siloxane functionalized PCSSi or SBSSi macromolecules on a Mg alloy surface clearly showed inhibition of initial thrombotic deposition and corrosion resistance compared to unmodified control surfaces in the acute stages of blood contact. The determination of the effect of the surface modification on protein adsorption, which would presumably be reduced with these modifying molecules,[16] was not possible in this study due to the rapid corrosion observed in the control samples. A simple, covalently bound silane layer on the Mg alloy surface might be sufficient to act as a means to prevent acute corrosion resistance, as some previous studies have indicated.[41,42] Further studies also would be needed to determine whether the inclusion of the PC and SB macromolecules on the silane base is critical in determining the degree of corrosion resistance observed. With the delayed, but inevitable, corrosion of the Mg alloy surface, the nonthrombogenic coating (PCSSi or SBSSi) would necessarily be removed over time. On the basis of the clinical risk period for acute thrombosis, where antithrombotic pharmaceutical therapy is more aggressive, it is presumed that the nonthrombogenic and corrosion resistance coating activity is most important in the first several days following device implantation. After this time, a slowly unmasked underlying and degrading alloy oxide surface would be better tolerated. Ultimately this phenomenon would need to be addressed with in vivo models for specific devices to verify the presumed benefit. The simple coating technology using functional PC or SB macromolecules could be also applied to many other nondegradable metallic cardiovascular devices including titanium alloys where thrombogenicity is similarly of concern such as vascular stents or ventricular assist devices.

5. CONCLUSIONS

Siloxane functional PC and SB macromolecules (PCSSi and SBSSi) were successfully prepared via a thiol-ene radical photopolymerization technique using UV irradiation and benzophenone as a photoinitiator. The functional PCSSi and SBSSi macromolecules could modify Mg alloy (AZ31) surfaces under anhydrous conditions. Acute platelet deposition and activation on the PCSSi- and SBSSi-modified alloy surfaces markedly decreased compared to those left unmodified. The PCSSi and SBSSi modified AZ31 also appeared to exhibit improved corrosion resistance. This simple and covalent modification pathway with functional PC or SB macromolecules could offer relative ease and effective application for complex surface shapes associated with (nondegradable) metallic cardiovascular devices as well as the growing number of investigational biodegradable Mg alloy devices.

AUTHOR INFORMATION

Corresponding Author

*(W.R.W.) E-mail: wagnerwr@upmc.edu.

Present Address

○Department of Bioengineering, University of Texas at Arlington, Arlington, Texas 76019, United States.

Notes

The authors declare no competing financial interest.

ACKNOWLEDGMENTS

This research was supported by the NSF Engineering Research Center for Revolutionizing Metallic Biomaterials (ERC-RMB) (Award #0812348, National Science Foundation). We would like to thank the Center for Biological Imaging (CBI) of the University of Pittsburgh for their kind assistance for the SEM images. J.W. was supported by the Cardiovascular Bioengineering Training Program (NIH Training Grant T32-HL076124). The surface analysis experiments done at NESAC/BIO were supported by NIH, NIBIB grant EB-002027.

REFERENCES

(1) Witte, F. The history of biodegradable magnesium implants: A review. *Acta Biomater.* **2010**, *6*, 1680−1692.

(2) Haude, M.; Erbel, R.; Erne, P.; Verheye, S.; Degen, H.; Böse, D.; Vermeersch, P.; Wijnbergen, I.; Weissman, N.; Prati, F.; Waksman, R.; Koolen, J. Safety and performance of the drug-eluting absorbable metal scaffold (DREAMS) in patients with de-novo coronary lesions: 12 month results of the prospective, multicentre, first-in-man BIOSOLVE-I trial. *Lancet* **2013**, *381*, 836−844.

(3) Erbel, R.; Di Mario, C.; Bartunek, J.; Bonnier, J.; de Bruyne, B.; Eberli, F. R.; Erne, P.; Haude, M.; Heublein, B.; Horrigan, M.; Ilsley, C.; Böse, D.; Koolen, J.; Lüscher, T. F.; Weissman, N.; Waksman, R. PROGRESS-AMS (Clinical performance and angiographic results of coronary stenting with absorbable metal stents) investigators. Temporary scaffolding of coronary arteries with bioabsorbable magnesium stents: a prospective, non-randomised multicentre trial. *Lancet* **2007**, *2* (369), 1869−1875.

(4) Erdmann, N.; Angrisani, N.; Reifenrath, J.; Lucas, A.; Thorey, F.; Bormann, D.; Meyer-Lindenberg, A. Biomechanical testing and degradation analysis of MgCa0.8 alloy screws: a comparative in vivo study in rabbits. *Acta Biomater.* **2011**, *7*, 1421−1428.

(5) Yang, J.; Cui, F.; Lee, I. S. Surface modifications of magnesium alloys for biomedical applications. *Ann. Biomed. Eng.* **2011**, *12*, 4250−4270.

(6) Hornberger, H.; Vitranen, S.; Boccaccini, A. R. Biomedical coatings on magnesium alloys: A review. *Acta Biomater.* **2012**, *8*, 2242−2455.
(7) Whelan, D. M.; Giessen, W. J.; Krabbendam, S. C.; Vliet, E. A.; Verdouw, P. D.; Serruys, P. W.; Beusekom, H. M. M. Biocompatibility of phosphorylcholine coated stents in normal porcine coronary arteries. *Heart* **2000**, *83*, 338−345.
(8) Galli, M.; Sommariva, L.; Prati, F.; Zerboni, S.; Politi, A.; Bonattie, R.; Mameli, S.; Butti, E.; Pagano, A.; Ferrari, G. Acute and mid-term results of phosphorylcholine-coated stents in primary coronary stenting for acute myocardial infaction. *Catheter Cardiovasc. Intervention* **2001**, *53*, 182−187.
(9) Kihara, S.; Yamazaki, K.; Litwak, P.; Kameneva, M. V.; Ushiyama, H.; Tokuno, T.; Borzelleca, D. C.; Umezu, M.; Tomioka, J.; Tagusari, O.; Akimoto, T.; Koyanagi, H.; Kurosawa, H.; Kormos, R. L.; Griffith, B. P. In vivo evaluation of MPC polymer coated continuous flow left ventricular assist system. *Artif. Organs* **2003**, *27*, 188−192.
(10) Zhang, J.; Yuan, J.; Yuan, Y. L.; Zang, X. P.; Shen, J.; Lin, S. C. Platelet adhesive resistance of segmented polyurethane film surface grafted with vinyl benzyl sulfo monomer of ammonium zwitterions. *Biomaterials* **2003**, *24*, 4223−4231.
(11) West, S. L.; Salvage, J. P.; Lobb, E. J.; Armes, S. P.; Billingham, N. C.; Lewis, A. L.; Hanlon, G. W.; Lloyd, A. W. The biocompatibility of crosslinkable copolymer coatings containing sulfobetaines and phosphobetaines. *Biomaterials* **2004**, *25*, 1195−1204.
(12) Snyder, T. A.; Tsukui, H.; Kihara, S.; Akimoto, T.; Litwak, K. N.; Kameneva, M. V.; Yamazaki, K.; Wagner, W. R. Preclinical biocompatibility assessment of the EVAHEART ventricular assist device: Coating comparison and platelet activation. *J. Biomed. Mater. Res.* **2007**, *81A*, 85−92.
(13) Sin, D. C.; Kei, H. L.; Miao, X. Surface coatings for ventricular assist devices. *Expert Rev. Med. Devices* **2009**, *6*, 51−60.
(14) Ye, S. H.; Johnson, C. A., Jr.; Woolley, J. R.; Snyder, T. A.; Gamble, L. J.; Wagner, W. R. Covalent surface modification of a titanium alloy with a phosphorylcholine-containing copolymer for reduced thrombogenicity in cardiovascular devices. *J. Biomed. Mater. Res., Part A* **2009**, *91*, 18−28.
(15) Ye, S. H.; Johnson, C. A., Jr.; Woolley, J. R.; Oh, H. I.; Gamble, L. J.; Ishihara, K.; Wagner, W. R. Surface modification of a titanium alloy with a phospholipid polymer prepared by a plasma-induced grafting technique to improve surface thromboresistance. *Colloids Surf., B* **2009**, *74*, 96−102.
(16) Ye, S. H.; Johnson, C. A., Jr.; Woolley, J. R.; Murata, H.; Gamble, L. J.; Ishihara, K.; Wagner, W. R. Simple surface modification of a titanium alloy with silanated zwitterionic phosphorylcholine or sulfobetaine modifiers to reduce thrombogenicity. *Colloids Surf., B* **2010**, *79*, 357−364.
(17) Ishihara, K.; Nomura, H.; Mihara, T.; Kurita, K.; Iwasaki, Y.; Nakabayashi, N. Why do phospholipids polymers reduce protein adsorption? *J. Biomed. Mater. Res.* **1998**, *39*, 323−330.
(18) Holmlin, R. E.; Chen, X.; Chapman, R. G.; Takayama, S.; Whitesides, G. M. Zwitterionic SAMs that resist nonspecific adsorption of protein from aqueous buffer. *Langmuir* **2001**, *17*, 2841−2850.
(19) Kitano, H.; Suzuki, H.; Matsuura, K.; Ohno, K. Molecular recognition at the exterior surface of a zwitterionic telomer brush. *Langmuir* **2010**, *26*, 6767−6774.
(20) Lecamp, L.; Houllier, F.; Youssef, B.; Bunel, C. Photoinitated cross-linking of a thiol-methacrylate system. *Polymer* **2001**, *42*, 2727−2736.
(21) Cramer, N. B.; Bowman, C. N. Kinetics of thiol-ene thiol-acrylate photopolymerizations with real-time Fourier transform infrared. *J. Polym. Sci., Part A: Polym. Chem.* **2001**, *39*, 3311−3319.
(22) Cramer, N. B.; Davies, T.; O'Brien, A. K.; Bowman, C. N. Mechanism and modeling of a thiol-ene photopolymerization. *Macromolecules* **2003**, *36*, 4631−4636.
(23) Hoyle, C. E.; Lee, T. Y.; Roper, T. Thiol-enes: Chemistry of the past with promise for the future. *J. Polym. Sci.* **2004**, *42*, 5301−5338.
(24) Zhang, B.; Wang, C.; Lang, L.; Cui, R.; Liu, X. Selective defect-patching of zeolite membrane using chemical liquid deposition at organic/aqueous interfaces. *Adv. Funct. Mater.* **2008**, *18*, 3434−3443.
(25) Johnson, C. A., Jr.; Snyder, T. A.; Woolley, J. R.; Wagner, W. R. Flow cytometric assays for quantifying activated ovine platelets. *Artif. Organs* **2008**, *32*, 136−145.
(26) Vojtěch, D.; Kubásek, J.; Šerák, J.; Novák, P. Mechanical and corrosion properties of newly developed biodegradable Zn-based alloys for bone fixation. *Acta Biomater.* **2011**, *7*, 3515−3522.
(27) Banerjee, P. C.; Raman, R. K. S. Electrochemical impedance spectroscopic investigation of the role of alkaline pre-treatment in corrosion resistance of a silane coating on magnesium alloy, ZE41. *Electrochim. Acta* **2011**, *56*, 3790−3798.
(28) Hoyle, C. E. Thiol-ene click chemistry. *Angew. Chem., Int. Ed.* **2010**, *49*, 1540−1573.
(29) Matsuno, R.; Takami, K.; Ishihara, K. Simple synthesis of a library of zwitterionic surfactants via Michael-type addition of methacrylate and alkane thiol compounds. *Langmuir* **2010**, *26*, 13028−13032.
(30) Zhou, F.; Liu, W.; Xu, T.; Liu, S.; Chen, M.; Liu, J. Preparation of silane-terminated polystyrene and polymethylmethacrylate self-assembled films on silicone wafer. *J. Appl. Polym. Sci.* **2004**, *92*, 1695−1701.
(31) Cook, W. D.; Chen, F.; Pattison, D. W.; Hopson, P.; Beaujon, M. Thermal polymerization of thiol-ene network-forming systems. *Polym. Int.* **2007**, *56*, 1572−1579.
(32) Tucker-Schwartz, A. K.; Farrell, R. A.; Garrell, R. L. Thiol-ene click reaction as a general route to functional trialkoxysilanes for surface coating applications. *J. Am. Chem. Soc.* **2011**, *133*, 11026−11029.
(33) Uygun, M.; Tasdelen, M. A.; Yagci, Y. Influence of type of initiation on thion-ene "click" chemistry. *Macromol. Chem. Phys.* **2010**, *211*, 103−110.
(34) Xue, D. C.; Yun, Y. H.; Schulz, M. J.; Shanov, V. Corrosion protection of biodegradable magnesium implants using anodization. *Mater. Sci. Eng., C* **2001**, *31*, 215−223.
(35) Lin, L.; Gao, J.; Wang, Y. Evaluation of cyto-toxicity and corrosion behavior of *alkali-heat-treated* magnesium in simulated body fluid. *Surf. Coat. Technol.* **2004**, *185*, 92−98.
(36) Gu, X. N.; Li, N.; Zhou, W. R.; Zheng, Y. F.; Zhao, X.; Cai, Q. Z.; Ruan, L. Corrosion resistance and surface biocompatibility of a microarc oxidation coating on a Mg−Ca alloy. *Acta Biomater* **2011**, *7*, 1880−1889.
(37) Gu, X. N.; Zheng, Y. F.; Cheng, Y.; Zhong, S. P.; Xi, T. F. In vitro corrosion and biocompatibility of binary magnesium alloys. *Biomaterials* **2009**, *30*, 484−498.
(38) Lu, P.; Cao., L.; Liu, Y.; Xu, X.; Wu, X. Evaluation of magnesium ions release, biocorrosion and hemocompatibility of MAO/PLLA-modified magnesium alloy WE42. *J. Biomed. Mater. Res., Part B* **2011**, *96*, 101−109.
(39) Hansi, C.; Arab, A.; Rzany, A.; Ahrens, I.; Bode, C.; Hehrlein, C. Differences of platelet adhesion and thrombus activation on amorphous silicon carbide, magnesium alloy, stainless steel, and cobalt chromium stent surfaces. *Catheter Cardiovasc. Intervention* **2009**, *73*, 488−496.
(40) Li, M.; Cheng, Y.; Zheng, Y. F.; Zhang, X.; Wei, S. C. Surface characteristics and corrosion behaviour of WE43 magnesium alloy coated by SiC film. *Appl. Surf. Sci.* **2012**, *258*, 3074−3081.
(41) Khramov, A. N.; Balbyshev, V. N.; Kasten, L. S.; Mantz, R. A. Sol−gel coatings with phosphonate functionalities for surface modification of magnesium alloys. *Thin Solid Films* **2006**, *514*, 174−181.
(42) Hu, J.; Li, Q.; Zhong, X.; Li, L.; Zhang, L. Organic coatings silane-based for AZ91D magnesium alloy. *Thin Solid Films* **2010**, *519*, 1361−1366.